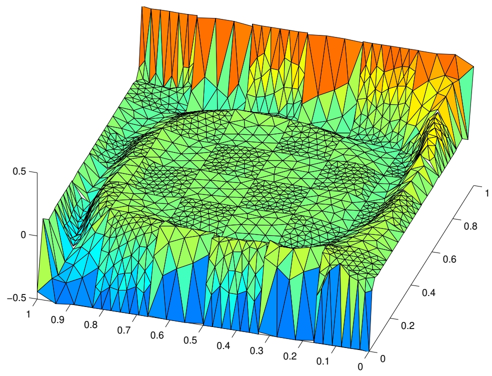

(a) stabilized three-field algorithm

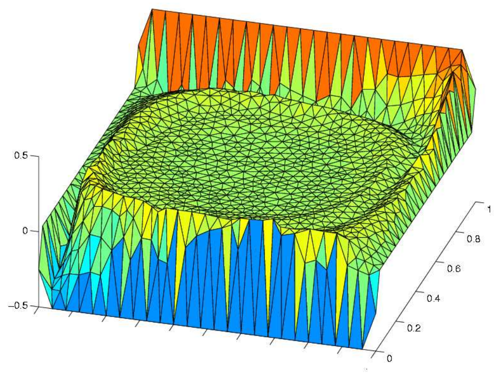

(b) computation with FEMLAB^{TM}

Figure 4.3: *The solution of Example 4.1 for $\epsilon = 10^{-6}$ computed in the multi-domain case using the stabilized three-field formulation (a) and with the help of* FEMLAB^{TM} *(b).*

with $\gamma_1 := \{(x_1, x_2) \in \partial\Omega \mid x_2 = 0\}$ and $\gamma_2 := \{(x_1, x_2) \in \partial\Omega \mid x_2 = 1\}$ and the flow $\mathbf{b}$ is defined by

$$\mathbf{b}(x_1, x_2) := \begin{pmatrix} (2x_2 - 1)(1 - (2x_1 - 1)^2) \\ 4x_2(2x_1 - 1)(x_2 - 1) \end{pmatrix}.$$

$\mathbf{b}$ *is a rotational flow with a center in $(\frac{1}{2}, \frac{1}{2})$ and $\nabla \cdot \mathbf{b} = 0$. Furthermore, $\mathbf{b} \cdot \mathbf{n} = 0$ holds on the whole boundary $\partial\Omega$.*

We decompose the unit square Ω into (6×6) squares. For the discretization the meshes of Figure 4.1 are chosen. The Lagrange multiplier meshes are chosen three times finer than the interior meshes. In the context of domain decomposition this example is particularly interesting. In the interior the solution is almost constant in the advection dominated case. The constant is given by the mean value of the Dirichlet data on the boundary. Now each discretization has to find this value by mixing the boundary information.
The result for $\epsilon = 10^{-6}$ is plotted in Figure 4.3 (a). In Figure 4.3 (b) the solution computed with the standard algorithm of FEMLAB^{TM} is plotted (mesh size $h = 0.04$). It can be seen that both plots are quite similar. So it can be stated that the proposed algorithm finds the correct interface values.

Verifying the h-convergence

Analogously to the single-domain case we have to check the theoretically predicted convergence rates. Again we consider the following smooth example:

Example 4.2 *Let the right hand side f and the boundary condition g be chosen in such a way that*

$$u(x, y) = x\cos(\pi y) \tag{4.31}$$

becomes the exact solution of

$$\begin{aligned} -\epsilon\triangle u + (-1, -1)^T \cdot \nabla u &= f \quad \text{in } \Omega \\ u &= g \quad \text{on } \Gamma. \end{aligned}$$

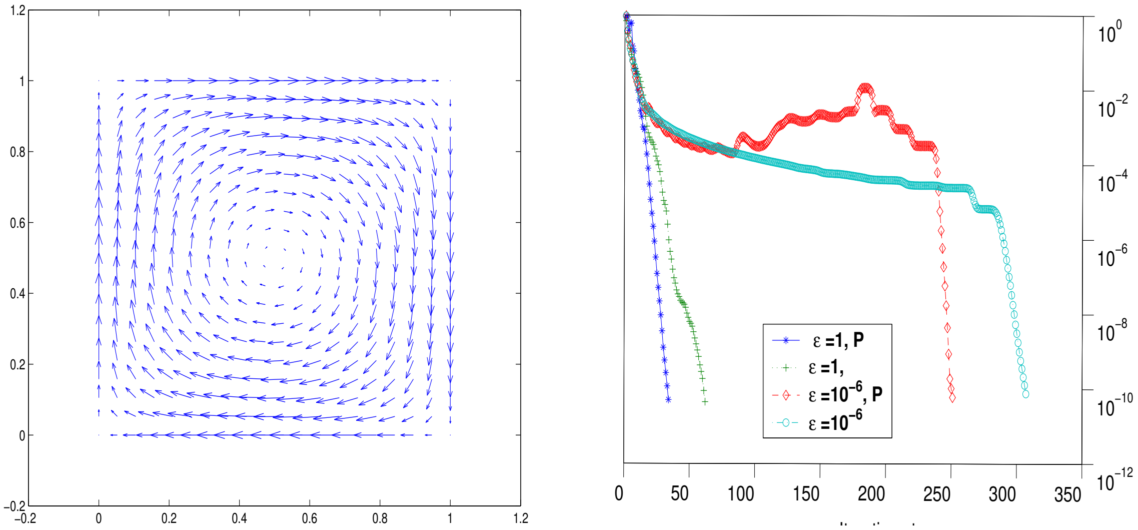

Figure 6.1: On the left hand side the flow $\mathbf{b}$ *of Example 4.1 is plotted. On the right hand side we see the residuum of the Schur complement equation for Example 4.1 in dependence on the iteration steps. 'P' denotes the preconditioned version. We use a* (3×3) *partition and the parameters are chosen by* $c = 10^{-7}$, $h = 0.005$.

convergence behavior: the number of iteration steps is almost independent of the mesh size. Quite different is the situation in the stabilized case. There, both algorithms depend on the mesh size and the preconditioned method works always worse. In addition, we clearly see the effect of the stabilization in the case without preconditioner. Due to the stabilization for $h = 0.005$ the number of iteration steps could be reduced by the factor 3.

The nonsymmetric case

Next we study the effect of the advection with the help of Example 4.1. Remember, that the given flow $\mathbf{b}$ is a rotational flow, where $\mathbf{b} \cdot \mathbf{n}$ vanishes on the whole boundary $\partial\Omega$ (cf. Figure 6.1). In addition, all characteristics are closed. As already discussed in section 4.3 solving this problem is extremely difficult for any domain decomposition method. Defining a global mesh size h the local mesh sizes are given by the checkerboard pattern (6.29). The stabilization parameters in this section are always given by the elliptic choice (6.28). For the Schur complement equation without preconditioner the constants of the stabilization parameters are determined by $\alpha_0 = 1$, $\beta_0 = 1$. Due to the results of the symmetric case for the preconditioned method we choose $\alpha_0 = 1$, $\beta_0 = 0.01$ in the diffusion dominated case and $\alpha_0 = 1$, $\beta_0 = 1$ in the advection dominated case.
In order to get an impression of the GMRES algorithm, the residuum in dependence on the iteration steps is plotted in Figure 6.1. In the advection dominated case we observe a stage, where the residuum almost stagnates. This behavior is typical for the GMRES method.
Let us consider Table 6.7. First, we observe, that we need much more iteration steps in the advection dominat regime. There, the structure of the problem is quite complicated. The solution possesses strong layers.
We observe, that the preconditioned method always needs less iteration steps for fine meshes than the method without preconditioner. But due to the preconditioning the number of iteration steps is only slightly reduced. Since the computation of the preconditioner is expensive, the application

for all $\phi \in H_*^{\frac{1}{2}}(\Gamma_i)$. Using the last representation of the algorithm by simple computations we arrive at

$$\begin{aligned}
&\epsilon \left\langle \lambda^i_{k+1}, \phi \right\rangle_{\Gamma_{ij}} + \langle f^-_{i,\Gamma_{ij}} \psi_{k+1}, \phi\rangle_{\Gamma_{ij}} \\
&\qquad \overset{(7.11)}{=} \epsilon\langle \lambda^i_{k+\frac{1}{2}}, \phi\rangle_{\Gamma_{ij}} - \langle f^+_{i,\Gamma_{ij}} u^i_{k+1} - f^+_{i,\Gamma_{ij}} \psi_{k+1} - f^-_{i,\Gamma_{ij}} \psi_{k+1}, \phi\rangle_{\Gamma_{ij}}
\end{aligned}$$

on the intersection Γ_{ij} of $\overline{\Omega_i}$ and $\overline{\Omega_j}$. Using the identity (7.10) yields

$$\begin{aligned}
\epsilon \left\langle \lambda^i_{k+1}, \phi \right\rangle_{\Gamma_{ij}} + \langle f^-_{i,\Gamma_{ij}} \psi_{k+1}, \phi\rangle_{\Gamma_{ij}} &= -\langle f^+_{i,\Gamma_{ij}} u^i_{k+1} - f^+_{i,\Gamma_{ij}} \psi_{k+1} - f^-_{i,\Gamma_{ij}} \psi_{k+1}, \phi\rangle_{\Gamma_{ij}} \\
- \Big(\epsilon\langle \lambda^j_{k+\frac{1}{2}}, \phi\rangle_{\Gamma_{ij}} &+ \langle -f^+_{i,\Gamma_{ij}} u^i_{k+1} - f^+_{j,\Gamma_{ij}} u^j_{k+1} + (f^+_{i,\Gamma_{ij}} + f^+_{j,\Gamma_{ij}})\psi_{k+1}, \phi\rangle_{\Gamma_{ij}} \Big) \\
&= -\epsilon\langle \lambda^j_{k+\frac{1}{2}}, \phi\rangle_{\Gamma_{ij}} + \langle f^+_{j,\Gamma_{ij}} u^j_{k+1} + (f^-_{i,\Gamma_{ij}} - f^+_{j,\Gamma_{ij}})\psi_{k+1}, \phi\rangle_{\Gamma_{ij}}
\end{aligned}$$

or

$$\begin{aligned}
\epsilon \left\langle \lambda^i_{k+1}, \phi \right\rangle_{\Gamma_{ij}} + \langle f^-_{i,\Gamma_{ij}} \psi_{k+1}, \phi\rangle_{\Gamma_{ij}} \quad \overset{(7.9)}{=} \quad & \langle f^+_{j,\Gamma_{ij}} u^j_{k+1} + (f^-_{i,\Gamma_{ij}} - f^+_{j,\Gamma_{ij}})\psi_{k+1}, \phi\rangle_{\Gamma_{ij}} \\
& - \Big(\epsilon\langle \lambda^j_k, \phi\rangle_{\Gamma_{ij}} - \langle f^-_{j,\Gamma_{ij}} u^j_{k+1} - f^-_{j,\Gamma_{ij}} \psi_k, \phi\rangle_{\Gamma_{ij}} \Big) .
\end{aligned}$$

In a next step we use the differential interpretation (7.7) of step (7.3) and insert the boundary condition on Γ_{ij}:

$$\begin{aligned}
&\epsilon \left\langle \lambda^i_{k+1}, \phi \right\rangle_{\Gamma_{ij}} + \langle f^-_{i,\Gamma_{ij}} \psi_{k+1}, \phi\rangle_{\Gamma_{ij}} \\
&= - \Big(\epsilon\langle \lambda^j_k, \phi\rangle_{\Gamma_{ij}} + \langle f^-_{j,\Gamma_{ij}} \psi_k, \phi\rangle_{\Gamma_{ij}} \Big) + \langle (f^+_{j,\Gamma_{ij}} + f^-_{j,\Gamma_{ij}}) u^j_{k+1} + (f^-_{i,\Gamma_{ij}} - f^+_{j,\Gamma_{ij}})\psi_{k+1}, \phi\rangle_{\Gamma_{ij}} \\
&= -\epsilon\langle \frac{\partial u^j_{k+1}}{\partial \mathbf{n}_j}, \phi\rangle_{\Gamma_{ij}} - \langle f^-_{j,\Gamma_{ij}} u^j_{k+1}, \phi\rangle_{\Gamma_{ij}} + \langle (f^+_{j,\Gamma_{ij}} + f^-_{j,\Gamma_{ij}}) u^j_{k+1} + (f^-_{i,\Gamma_{ij}} - f^+_{j,\Gamma_{ij}})\psi_{k+1}, \phi\rangle_{\Gamma_{ij}} \\
&= \left(\epsilon\langle \frac{\partial u^j_{k+1}}{\partial \mathbf{n}_i}, \phi\rangle_{\Gamma_{ij}} + \langle f^-_{i,\Gamma_{ij}} u^j_{k+1}, \phi\rangle_{\Gamma_{ij}} \right) + \left\langle (f^-_{i,\Gamma_{ij}} - f^+_{j,\Gamma_{ij}})(\psi_{k+1} - u^j_{k+1}), \phi \right\rangle_{\Gamma_{ij}} . \qquad (7.12)
\end{aligned}$$

Using assumption (7.2) and again the representation (7.7) we obtain the assertion by

$$\begin{aligned}
\epsilon\langle \frac{\partial u^i_{k+2}}{\partial \mathbf{n}_i}, \phi\rangle_{\Gamma_{ij}} + \langle f^-_{i,\Gamma_{ij}} u^i_{k+2}, \phi\rangle_{\Gamma_{ij}} \quad &= \quad \epsilon \left\langle \lambda^i_{k+1}, \phi \right\rangle_{\Gamma_{ij}} + \langle f^-_{i,\Gamma_{ij}} \psi_{k+1}, \phi\rangle_{\Gamma_{ij}} \\
&= \quad \epsilon\langle \frac{\partial u^j_{k+1}}{\partial \mathbf{n}_i}, \phi\rangle_{\Gamma_{ij}} + \langle f^-_{i,\Gamma_{ij}} u^j_{k+1}, \phi\rangle_{\Gamma_{ij}} .
\end{aligned}$$

□

Remark 7.3 *Unfortunately in the discrete case for nonmatching grids the assumption (7.2) is in general not fulfilled. But then the equation (7.12) on the interface Γ_{ij} gives*

$$\begin{aligned}
\epsilon\langle \frac{\partial u^i_{k+2}}{\partial \mathbf{n}_i}, \phi\rangle_{\Gamma_{ij}} + \langle f^-_{i,\Gamma_{ij}} u^i_{k+2}, \phi\rangle_{\Gamma_{ij}} &= \left\langle (f^-_{i,\Gamma_{ij}} - f^+_{j,\Gamma_{ij}})(\psi_{k+1} - u^j_{k+1}), \phi \right\rangle_{\Gamma_{ij}} \\
&\quad + \epsilon\langle \frac{\partial u^j_{k+1}}{\partial \mathbf{n}_i}, \phi\rangle_{\Gamma_{ij}} + \langle f^-_{i,\Gamma_{ij}} u^j_{k+1}, \phi\rangle_{\Gamma_{ij}} \quad \phi \in \Phi.
\end{aligned}$$